

A laser beam machining (LBM) database for the cutting of ceramic tile

I. Black *, S.A.J. Livingstone, K.L. Chua

Department of Mechanical and Chemical Engineering, Heriot-Watt University, Riccarton, Edinburgh EH14 4AS, UK

Received 13 December 1997

Abstract

This paper covers the cutting of commercially-available ceramic tiles using a CO₂ laser cutting machine, with the object of producing a laser beam machining (LBM) database that contains the essential parameter information for their successful processing. Various laser cutting parameters were investigated that would generate a cut in ceramic tile which required minimal post-treatment. The effects of various shield gases, of multi-pass cutting and of underwater cutting were also examined. © 1998 Elsevier Science S.A. All rights reserved.

Keywords: CO₂; Laser cutting; Ceramic materials; Advanced manufacturing processes

1. Introduction and background

Manual methods of cutting ceramic tiles are very similar to that for glass, i.e. scribing the materials with tungsten-carbide tipped cutter, followed by the application of a bending moment along the scribed line to initiate controlled fracture. However, manual techniques are limited to straight-line cutting and relatively large-radius cuts. Internal and undercut profiles are nearly impossible to produce with scoring alone (with the possible exception of internal circles); more sophisticated methods having to be applied to achieve these profiles. Traditionally, diamond-saw, hydrodynamic (water jet) or ultrasonic machining are used to create complex geometries in ceramic tiles, but these processes are very time consuming and expensive. For example, typical diamond-saw cutting speeds are in the order of 20 mm min⁻¹ [1], while ultrasonic drilling of Al₂O₃ takes over 30 s per hole [2].

The most critical factor arising from use of a CO₂ laser to cut ceramic tiles is crack damage, which is essentially caused by a high temperature gradient within the ceramic substrate during the cutting process. These cracks reduce the strength and are sources for

critical crack growth, which may result in partial or complete failure of the tile substrate [3]. Thus a reduction of process-induced crack formation is paramount for the realistic commercial use of lasers to cut ceramic tiles.

2. Laser cutting parameters

Laser machining of any material is a complex process involving many different parameters that which all need to work in consort to produce a quality machining operation [4], parameters such as: (i) laser power input; (ii) focal setting; (iii) assist gas type and pressure; (iv) nozzle configuration; (v) workpiece thickness; and (vi) optophysical properties.

Previous research within the authors' department [1,5,6] has also demonstrated the criticality of the above parameters in efficient laser cutting.

2.1. Laser power

Laser power depends on the type of laser used. For the work reported in this paper, a Ferranti MF400 CNC laser cutter was employed, rated at a power output of 400 W. However, due to upgrading, the maximum beam power achievable was between 520 and

* Corresponding author. Fax: +44 131 4513129; e-mail: i.black@hw.ac.uk

530 W in continuous wave (CW) cutting mode. The laser also had the ability to work in pulse mode (PM) and super-pulse mode (SPM; Fig. 1). To determine the equivalent power output during pulsing operation, a power verses pulsing chart was used in conjunction with the following basic equation [9]:

$$Pr = Pl/Ps$$

$$f = 1/(Pl + Pr)$$

Although the laser cutter could operate between frequencies of 50 and 5000 Hz, a value of 500 Hz was recommended in previous work [1,5]. Since this setting proved to be successful, only limited investigation into other frequencies was carried out (at 250 Hz, 750 and 100 Hz).

2.2. Cutting speed

The CNC table used with the Ferranti MF400 laser cutter had a maximum feed rate of 10000 mm min⁻¹. Previous work [6] indicated that feed rates above 6000 mm min⁻¹ proved to be unstable for any standardised testing. The optimum cutting speed varied with the power setting and, more importantly, with the thickness of the workpiece.

2.3. Shield gas type and pressure

Compressed air, argon, nitrogen and oxygen were used as shield gases during cutting, with $p_{\max} \approx 4$ bar. Different shield gases were used to examine their effect on cut quality after processing, since the shield gas not only cools and cut edges and removes molten material, but also generates a chemical reaction with the substrate material [7]. The results of this chemical reaction differ for each type of shield gas used. For test purposes p was varied in steps of 0.5 bar from 1 to 2.5 bar, then in steps of 0.2 bar from 2.6 bar to the maximum attainable gas pressure.

2.4. Nozzle configuration

The nozzle diameter contributes directly to the maximum achievable gas pressure and hence to the mass flow rate of the gas was important for the economics of cutting, especially when using cylinders of argon and nitrogen. Only circular profiles for the nozzle exits were available ($0.6 \text{ mm} \leq N_s \leq 20 \text{ mm}$), but this uniform nozzle exit geometry allowed cutting in any direction.

2.5. Nozzle height and focal positioning

The height at which the nozzle was set was governed by the position of the focal point. The Ferranti MF400 laser cutter only possessed a long focal length of 110

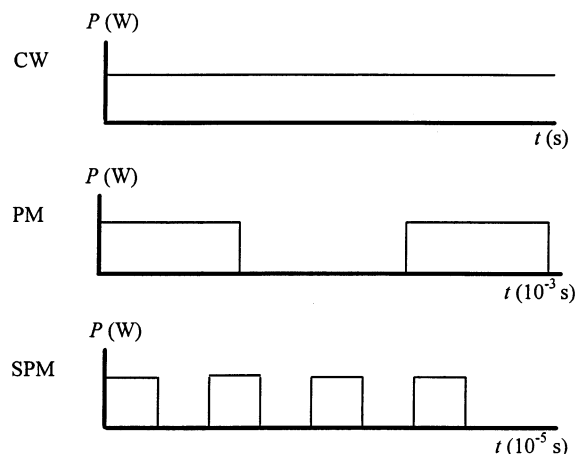


Fig. 1. Cutting modes.

mm (originally a short focal length of 46 mm was available before upgrading) and this length could be altered by ± 5 mm. If the nozzle height was incorrectly set the beam would 'clip' the nozzle and reduce the equivalent power output to the workpiece [6]. For the bulk of the testing the focal height was set so the focal point was 'on the job', i.e. on the top surface of the workpiece. This condition obviously governed the position of the nozzle above the workpiece.

3. Experimental procedure

Six types of Si/Al₂O₃-based ceramic tiles were examined (Table 1), originating from different countries. Note that the composition of the tiles varied, as did the thickness, but all possessed a surface glaze and in the case of the 7.5, 8.6 and 9.2 mm Spanish tiles the glaze was double layered.

3.1. Set-up procedure

Since there was a need for standard testing conditions, the following procedure was implemented before the start of testing: (i) the beam power was validated to specification, i.e. 520–530 W developed at full power (CW), although this dropped to around 50 W after

Table 1
Types of ceramic tile used

Tile type	Body colour	t_s (mm)
Brazilian	White	3.7
Peruvian	White	4.7
Italian	Light red	5.2
Spanish	Red	5.74
Spanish	Red	7.5
Spanish	Red	8.6
Spanish	Red	9.2

about 1 h of testing; (ii) the nozzle and the focal lens were checked to ensure that they were in good condition, i.e. clean and undamaged; (iii) the shield gas pressure regulator and shield gas tanks were turned on to prevent damage to the focal lens; (iv) the laser beam was centred within the nozzle using a 'square test', a lower energy input in PM being used to cut a square on a mild steel, the sparking density that resulted from cutting being checked to see if it was equally distributed about the cut line; and (v) the focal point was set for its desired positioning, i.e. 'on the job'.

3.2. Testing

A straight-line test (SLT) was used to evaluate the variable laser parameters for full through-cutting (FTC). Angular cutting was configured to investigate how the material reacted during cutting of tight geometry. Circular testing and square testing were devised to determine the effects resulting from cutting various geometries.

The SLT allowed for the combined testing of two separate parameters on one testpiece, upon completion the results being present automatically in a 'cutting matrix' in the form of the resulting cuts. P and V are the most important laser parameters, as they dictate the amount of energy input per unit length of cut, therefore they were paired for the SLT, as were p and N_s which govern the mass flow rate of the shield gas.

For the P/V test runs, the power was held constant while the cutting speed was increased along the cut (Fig. 2(a)). The length of cut at constant cutting speed had to be of sufficient magnitude to accommodate the acceleration or deceleration of the CNC table between feed changes: previous work [6] indicated that 50 mm was adequate. Interpreting the results was made easier due to their tabular format, with the 'cutting matrix' showing clearly any trends or patterns occurring due to the changes in parameter settings. The SLT also allowed a large number of cuts to be carried out over a short time-frame. This proved advantageous, as the laser tended to drift from its initial settings with time. Precautions had to be taken to avoid localised heating in the tile from continuous close proximity cutting, as a change in tile body temperature would invalidate any resulting data. Initially, a 20 mm separation between cuts was used and this proved sufficient. In order to study how close the cuts could be made to each other, the separation between cuts was reduced by increments of 2 mm from an initial 20 mm spacing.

During the SLT the other laser parameters had to be held constant [6]. For P versus V , f was held at 500 Hz with $N_s = 1.2$ mm and $p = 3$ bar. The beam focal point remained on the job. The results from the P/V cutting matrix determined the fixed values for the cutting speed and pulse settings for the succeeding SLT. For the N_s/p

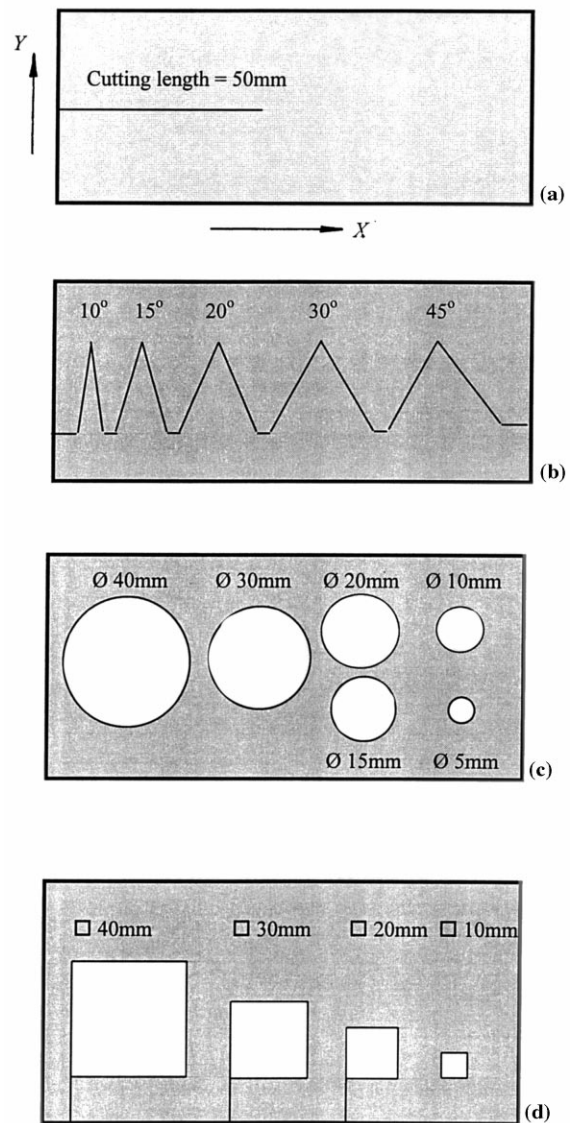


Fig. 2. Testing configuration: (a) straight-line testing; (b) angular testing; (c) circular testing; (d) square testing.

cutting matrix, the nozzle size remained constant along the x -axis (refer to Fig. 2(a)) while p was increased in steps of 0.2 bar from 2 bar in the y -axis (the cut separation remained constant at 20 mm). A new matrix was created subsequently for each nozzle size.

Angular testing (Fig. 2(b)) was used to investigate how the cut material reacted to sustained exposure from the laser beam during the machining of 'tight' geometries (i.e. where several cuts are made in close proximity to each other). The proximity test mentioned for SLT determines how close parallel lines can be cut to each other, whereas angular testing is used to determine how the cutting of acute angles effects the cut quality. The angles cut from a workpiece were reduced from 45° to 10° and the corresponding surface finish quality (SFQ) was noted.

Table 2
Multi-pass cutting parameters

Cutting mode	P_l	P_s	No. of passes	Last cut
CW	—	—	60	FTC
SPM	100	9000	100	FTC

There are two reasons for conducting square and circular testing (Fig. 2(c) and (d)): first, to determine the optimum method of laser-beam introduction to internal cut profiles; and secondly, to determine if there was any limitation in the dimension of the size of square or hole cut. If not correctly introduced, the laser beam would cause an internally-cut profile to fail at the point of introduction, due to the brief but excessive thermal gradient induced from cutting (i.e. thermal shock). Therefore, utilising methods of beam introduction, such as trepanning, onto a profile enabled complex geometries to be investigated. What also became apparent during testing was the importance of the position of beam extraction from the cut profile and the position of the beam starting point relative to the geometry, i.e. whether it was at a corner or on a straight edge.

3.3. Multi-pass and underwater cutting

Multi-pass cutting was begun with a low power ($P = 100$ W) laser beam. The first pass produced a well defined blind kerf in the substrate, followed by a second pass to cut deeper and so on. The process was repeated until the kerf was about 20 mm deep and then the laser power was switched to 500 W and do the final FTC. The objective of multi-pass cutting was to reduce thermal overload by use of less input energy per unit length. The parameters used in this test are given in Table 2.

Table 3
Grading of SFQ

Grading	
1	No cracking in surface glaze, solid sharp cut edge
2	Minimal glaze cracking ($W_c < 2$ mm) with slight loss of sharpness in cut edge
3	Medium cracking ($2 \text{ mm} < W_c < 4$ mm) and slight damage to unglazed tile substrate
4	Significant damage to glaze coating ($W_c > 6$ mm), heavy damage to unglazed substrate causing flaking in the glazed surface
5	Same as 4 but with the formation of cracks in the tile's main body leading to structural failure in a part of the tile (usually at the end of a cut or within 8 mm of the tile edge).

Underwater cutting was conducted with the objective of reducing the influence of heat around the cut area and also to examine the effect on cut quality through accelerated heat dissipation using water [8]. The ceramic tile was placed under water and the nozzle was also dipped in water, the shield gas pressure preventing any water from entering the nozzle jet chamber.

4. Cut quality

Material properties, laser parameters and workpiece geometry have a significant effect on the final result of the laser cutting process. Cut quality is essentially characterised by surface roughness and dross height, whereas crack length dictates the strength reduction in the substrate (Fig. 3). The overall SFQ at the glaze surface was classified according to the grading scale given in Table 3. Therefore, the quality of the cut surface and edge were measured with respect to: (i) surface roughness; (ii) surface finish and; (iii) dross adherence.

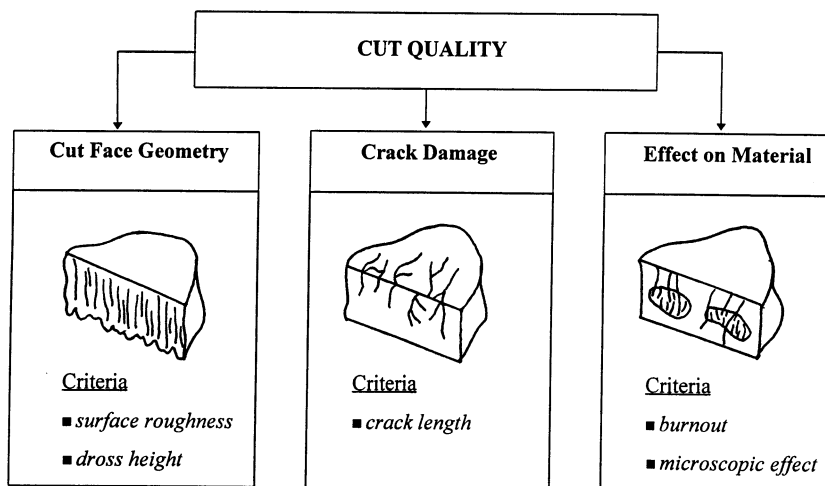


Fig. 3. Quality criteria for the laser cutting of ceramic tiles.

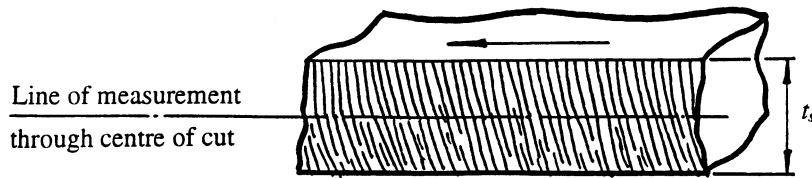


Fig. 4. Measurement of R_a for the cut surface.

4.1. Surface roughness

It was important to measure surface roughness as this allowed the cut quality to be gauged alongside values obtained from previous work [1] and values recorded for other manufacturing processes. Due to the large number of cuts being made it was necessary to reduce the number of cuts to be analysed. Therefore cuts with $SFQ < 2$ were not measured.

The surface roughness of the cut edge was characterised by the formation of striation lines left by the cutting process. R_a values were measured from the centre-line of the cut edge (Fig. 4). Measurements were taken over a 12.5 mm traverse of the stylus with a cut-off value of 2.5 mm, i.e. five readings were taken over the traverse, which ensured that the stylus travelled over a reasonable number of striation lines.

4.2. Dross adherence

Dross adherence directly effected the R_a value of the cut and the ability to remove internally-cut geometries. A micrometer was used to measure the dross height at three intervals along the cut section. The dross height remained fairly constant (approximately 1 mm) with all types of cutting. Since this value was deemed to be of no practical importance, it was not recorded in the database.

5. Results

Table 4 contains the current LBM database for cutting ceramic tiles that was compiled from the results of the work reported in this paper. The first part of the table contains the parameters and results for substrates cut in atmosphere, while the results for underwater cutting are shown in the second part.

5.1. Parameter effects

5.1.1. Cutting speed

For the thinner tiles ($t_s < 7$ mm) the P/V cutting matrix showed a wide region of FTC with $SFQ = 1$. In the case of the Brazilian tile ($t_s = 3.7$ mm) FTC was obtained with cutting speeds of up to 2200 mm min^{-1} and down to $Pr = 0.5$ (with reduced speeds) at $f = 500$

Hz. This region diminished with the increase in tile thickness and also with the redness of the body colour (generally the thicker tiles are darker in body colour). Fig. 5 shows how the maximum cutting speed for FTC varies with t_s . The 'exponential' relationship obtained concurs with previous work [6] for different materials such as steel, wood and perspex. The cutting matrix also showed that once the cutting speed exceeded values for attainable FTC, scribing or blind cutting results.

5.1.2. Pulsing

Pulsing the laser for all but the thick Spanish tiles was not required, as the CW setting produced cuts with a good SFQ grading. Successful FTC was obtained at $Pr \geq 0.4$ in the Brazilian tile, but V_{\max} was so low that, in a practical sense, the settings were not viable. On the thick Spanish tiles pulsing of the beam was required, as CW caused cracking in the glaze. This was probably due to an excess of energy input per unit length of cut causing thermal shock as the thermal expansion rate of the glaze differed sufficiently from that of the parent tile. Since pulsing the laser reduced the energy input by approximately 25 W for every 0.1 drop in Pr at $f = 500$ Hz, the surface glaze cracking virtually disappeared at $Pr = 0.6$ and optimum cutting speed, although tiny cracks (of the order of 0.5 mm wide) at the cut edge still remained.

5.1.3. Gas pressure

This parameter has a great effect on the quality and the rate at which cuts could be made successfully. Previous work [2] had shown that high gas pressures were required to achieve FTC on thick substrates ($t_s > 7$ mm). This was borne out by the results obtained from the p/N_s cutting matrix. High quality cuts were achieved in the thinner tiles ($t_s < 6$ mm) at gas pressures of 2 bar but in the double-glazed, thicker tiles values of $SFQ < 3$ were not achieved unless $p > 3$ bar. At low pressures ($p < 2.5$ bar), the maximum cutting speeds for FTC dropped drastically, as the gas failed in its role of dross clearer. V_{\max} for Brazilian tile in CW dropped from 2200 mm min^{-1} at $p = 3.8$ bar to 1500 mm min^{-1} at $p = 3$ bar. An increase in surface-glaze cracking also became apparent at low gas pressures. This led to the conclusion that the shield gas was acting as a coolant and thus helping to minimise the large thermal gradient created by the beam.

Table 4
4 LBM database for ceramic tiles

Atmospheric cutting												
Tile type	t_s (mm)	Body colour	Glaze type	Geometric cut	$Pl-Ps$	V (mm/min)	Shield gas	p (bar)	N_s (mm)	SFQ	R_a (μm)	
Brazilian	3.7	White	White	Straight	CW	500–1000	C. air	>3	1.2–1.5	1	25–35	
					180–20	500–1000	C. air	>3	1.2–1.5	1	25–35	
					160–40	500–900	C. air	>3	1.2–1.5	1	25–35	
				Internal	180–20	400–600	C. air	>3	1.2–1.5	1	25–35	
					Angular	160–40	300–500	C. air	>3	1.2–1.5	1–5	25–35
					Radial	180–20	300–500	C. air	>3	1.2–1.5	1	25–35
Peruvian	4.7	White	White	Straight	CW	500–700	C. air	>3	1.2–1.5	1	25–35	
					180–20	500–700	C. air	>3	1.2–1.5	1	25–35	
					160–40	500–700	C. air	>3	1.2–1.5	1	25–35	
				Internal	180–20	300–500	C. air	>3	1.2–1.5	1	25–35	
					Angular	160–40	250–450	C. air	>3	1.2–1.5	1–5	25–35
					Radial	180–20	250–450	C. air	>3	1.2–1.5	1	25–35
Italian	5.2	Light red	White	Straight	CW	500–700	C. air	>3	1.2–1.5	1	17–25	
					180–20	500–700	C. air	>3	1.2–1.5	1	17–25	
					160–40	500–700	C. air	>3	1.2–1.5	1	17–25	
				Internal	180–20	300–500	C. air	>3	1.2–1.5	1	17–25	
					Angular	160–40	200–400	C. air	>3	1.2–1.5	1–5	17–25
					Radial	180–20	200–400	C. air	>3	1.2–1.5	1	17–25
Spanish	5.74	Red	White	Straight	CW	300–550	C. air	>3	1.2–1.5	1	20–30	
					180–20	300–400	C. air	>3	1.2–1.5	1	20–30	
					160–40	300–450	C. air	>3	1.2–1.5	1	20–30	
				Internal	180–20	200–350	C. air	>3	1.2–1.5	1	20–30	
					Angular	160–40	200–300	C. air	>3	1.2–1.5	2–5	20–30
					Radial	180–20	200–350	C. air	>3	1.2–1.5	1	20–30
Spanish	7.5	Red	Clear/white	Straight	CW	200–370	C. air	>3	1.2–1.5	2	16–37	
					180–20	200–350	C. air	>3	1.2–1.5	2	16–37	
					160–40	200–350	C. air	>3	1.2–1.5	1–2	16–37	
				Internal	140–60	200–350	C. air	>3	1.2–1.5	2	16–37	
					Angular	140–60	200–300	C. air	>3	1.2–1.5	1–2	16–37
					Radial	140–60	200–250	C. air	>3	1.2–1.5	3–5	16–37
Spanish	8.5	Red	White	Straight	100–250	30–70	Argon	2.8	1.2	1	9–12	
					100–200	30–80	Argon	2.8	1.2	1	9–11	
					100–300	30–40	Argon	2.8	1.2	1	12–13	
				Internal	150–250	30–80	Argon	2.8	1.2	1	10–14	
					100–200	70–80	Argon	2.8	1.2	1	—	
					150–250	50–70	Argon	2.8	1.2	1	—	
				Straight	CW	150–250	Argon	2.2	1.2–1.5	3	—	
					180–20	150–250	Argon	2.2	1.2–1.5	3	4–6	
					180–30	150–250	Argon	2.2	1.2–1.5	2–4	4–8	
					180–40	150–250	Argon	2.2	1.2–1.5	2–4	6–9	
					180–50	150–250	Argon	2.2	1.2–1.5	2–4	7–11	
					160–20	150–250	Argon	2.2	1.2–1.5	3	9–11	
					160–30	150–250	Argon	2.2	1.2–1.5	3	10–11	
					160–40	150–250	Argon	2.2	1.2–1.5	3	11–13	
Straight	140–20	150–200	Argon	2.2	1.2–1.5	2	10–12					
	140–40	150–200	Argon	2.2	1.2–1.5	3	10–14					
	140–60	150–200	Argon	2.2	1.2–1.5	3	10–14					
	150–250	50	C. air	3.5	1.2	1	7–9					
	100–250	30–50	C. air	3.5	1.2	1	7–8					
	100–200	50–70	C. air	3.5	1.2	1	10–12					
	100–200	60–80	C. air	3.5	1.2	1–2	—					
Straight	CW	70–160	Nitrogen	3.5	1.2	3	15–18					
	150–250	40–60	Nitrogen	3.5	1.2	1	9–12					
	100–250	30–50	Nitrogen	3.5	1.2	1	8–10					
	100–200	20–50	Nitrogen	3.5	1.2	1	9–11					

Table 4 (continued).

Atmospheric cutting												
Tile type	t_s (mm)	Body colour	Glaze type	Geometric cut	PI - Ps	V (mm/min)	Shield gas	p (bar)	N_s (mm)	SFQ	R_a (μm)	
Spanish	9.2	Red	White	Angular	150–250	40–60	Nitrogen	3.5	1.2	3–4	—	
					100–250	30–40	Nitrogen	3.5	1.2	3–4	—	
					CW	80–100	Oxygen	3.5	1.2	3	—	
				Straight	100–200	50–60	Oxygen	3.5	1.2	1	10–11	
					100–250	30–50	Oxygen	3.5	1.2	1	9–11	
					150–250	30–80	Oxygen	3.5	1.2	1	10–12	
				Angular	150–250	70–80	Oxygen	3.5	1.2	1–3	—	
					100–250	50	Oxygen	3.5	1.2	1–3	—	
					150–200	40–100	C. air	3.5	1.2	1	10–13	
				Straight	100–200	30–40	C. air	3.5	1.2	1	9–10	
					100–250	20–30	C. air	3.5	1.2	1	10–12	
					150–250	30–100	C. air	3.5	1.2	1	10–12	
					Angular	150–200	40–80	C. air	3.5	1.2	1–4	—
						100–200	30–40	C. air	3.5	1.2	1–4	—
						100–250	20–30	C. air	3.5	1.2	1–4	—
150–250	40–80	C. air	3.5		1.2	1–4	—					
Underwater Cutting												
Spanish	8.5	Red	White		10° acute	100–200	50	Oxygen	3.5	1.2	1–2	
				100–250		50	Oxygen	3.5	1.2	1–2		
				150–250		50	Oxygen	3.5	1.2	1–2		
Spanish	9.2	Red	White	10° acute	100–200	50	Oxygen	3.5	1.2	1–2		
					100–250	50	Oxygen	3.5	1.2	1–2		
					150–250	50	Oxygen	3.5	1.2	1–2		

Note: focal point on the job; data for angular cut only.

5.1.4. Gas type

Compressed air as recommended by previous work [1] proved adequate in the removal of molten material without any adverse effects from its exothermic properties, over the full range of tile thicknesses. Cutting using the inert gases argon and nitrogen produced better results, especially with the latter as it acted as an efficient coolant [9]. High-quality cuts with SFQ = 1 were produced in the thicker tiles at an optimum cutting speed of 360 mm min⁻¹ in CW mode. However, when using the required high gas pressures, a cylinder of nitrogen or argon was used quickly.

5.1.5. Nozzle size

This parameter was related directly to p (i.e. the smaller is the nozzle size the higher is the obtainable pressure). Table 5 shows the maximum achievable shield gas pressure with the corresponding nozzle sizes when using compressed air. Nozzles with diameters greater than 1.5 mm were ignored as p_{max} was insufficient. The smaller nozzle diameters produced better cuts with higher cutting speeds.

5.1.6. Focal point positioning

During testing the focal point of the beam remained on the job, i.e. on the surface. Cuts with an adequate SFQ grading were achieved with this setting. Investiga-

tion showed that by lowering the focal point into the job the 'dross' adherence decreased and in raising the focal point away from the job FTC was lost as the beam de-focused. Therefore, for practical reasons, the focal point remained on the job.

5.1.7. Multi-pass cutting

Thicker tiles were cut successfully by the multi-pass method without degradation of cut quality. Due to the low power of the laser beam, the temperature gradient in the tile was greatly reduced, thus material damage was minimised. This method can also be used to process thicker ceramics without any fracture. However, multi-pass cutting has a distinct disadvantage in being a very time-consuming process and would prove uneconomic on a commercial basis.

5.2. Material effects

The darker-bodied tiles were denser and heavier and during cutting they retained more heat than the white-body tiles. Analysing how this effected the cutting was not possible, as the thickness of tile also increased with darkening of the body colour, the increase in thickness masking any of the compositional effects of the material. In some of the tiles the material composition was not homogeneous. Whether this was due to the specific

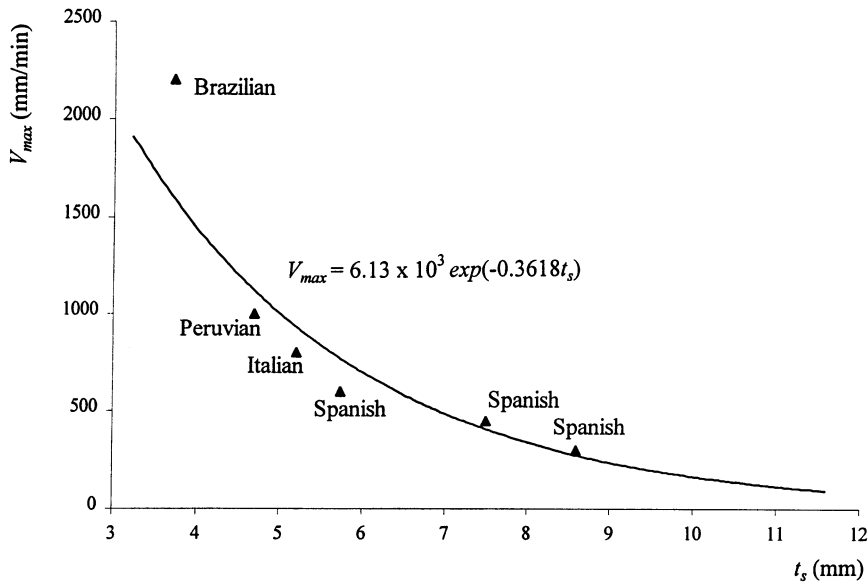


Fig. 5. V_{\max} against t_s for ceramic tiles of different origin.

tile manufacturing processes is unknown, but the results on cutting were a loss of FTC even at optimum cutting speed.

Glaze damage was a significant factor in assessing cut quality. In all but the thicker tiles glaze damage was minimal even at poor parameter settings. For example, with the 7.5 mm Spanish tile $SFQ \leq 3$ for most of the cuts with compressed air, although nitrogen produced better values. The problem with this latter type was that the tile had a double-layered glaze. No cracking appeared in the lower white glaze (similar to the other tiles) but the upper clear glaze splintered and flaked if the energy input or heat retention in the tile was too high. Barbero, Kaufman and Idelsohn [10] have shown that the surface glaze usually possesses a different linear expansion rate to that of the underlying substrate. Therefore the large thermal gradient caused by the laser beam causes the lower substrate to expand at a different rate, resulting in cracking of the glaze.

Another significant factor was control of the amount of energy input and heat dispersion from the cut. The effects of poor parameter settings were either loss of

FTC (which was corrected easily), or thermal shock in the tile or the surface glaze (i.e. cracking in the glaze). The laser cutting process readily promoted thermal shock during cutting, so it was vital to control this effect with the correct selection of parameters. The thermal properties of ceramic tile were primarily the cause of the problem, as generally a tile has a poor thermal conductivity ($0.9 \text{ W mK}^{-1} \leq k \leq 1 \text{ W mK}^{-1}$) and a relatively low co-efficient of expansion ($2 \times 10^{-6} \text{ K}^{-1} \leq \alpha \leq 5 \times 10^{-6} \text{ K}^{-1}$).

The glassy film (or dross) that covered the cut edge thickened with an increase in tile substrate and reduction in cutting speed. The increase in dross due to tile thickness was obvious: more tile melted, therefore more dross resulted. The thickness of the dross film also varied through the cut. There were two apparent reasons for this.

(a) First, the width of the beam diverged after the focal point (which was on the job), thus causing an out-of-flatness in the cut which resulted in a larger kerf width at the bottom. Therefore, more of the parent tile material was melted lower down in the cut. Depending on the laser focal length and positioning of the focal point, the kerf width varied from the focal spot size (approximately 0.1 mm) to 2 mm.

(b) Second, the ability or inability of the shield gas to remain as a focused jet through the cut also dictated the pattern of dross on the cut edge. At the top of the cut where the gas pressure was still high and the gas flow was still directed, little or no dross adherence was evident, but as the depth of cut increased the gas flow became more turbulent, reducing pressure and so allowing more dross to adhere to the cut edge.

Table 5
Maximum pressures (for compressed air) with varying nozzles sizes

N (mm)	p_{\max} (bar)
1.1	4
1.2	3.8
1.4	3.5
1.5	3.1
1.8	2.5

6. Nomenclature

f	pulse frequency (Hz)
k	thermal conductivity (W mK^{-1})
N_s	nozzle diameter (mm)
P	laser beam power (W)
Pl	pulse length (s)
P_s	pulse separation (s)
Pr	pulse ratio
p	shield gas pressure (bar)
p_{\max}	maximum shield gas pressure (bar)
R_a	surface roughness (μm)
t	time (s)
t_s	substrate thickness (mm)
V	cutting speed (mm min^{-1})
V_{\max}	maximum cutting speed (mm min^{-1})
W_c	surface glaze crack width (mm)
<i>Greek letter</i>	
α	linear coefficient of expansion (1 K^{-1})

Acknowledgements

The authors would like to express their thanks to the staff of the Advanced Manufacturing Unit of the Department of Mechanical and Chemical Engineering, Heriot-Watt University, for both their invaluable con-

tribution to the work detailed in this paper and their permission to publish the results.

References

- [1] B.E. Brath, CO₂ laser cutting of ceramic tile, Beng. dissertation, Heriot-Watt University, Edinburgh, UK, 1994.
- [2] G. Chryssolouris, Laser Machining: Theory and Practice, Springer, Berlin, 1991.
- [3] H.K. Tönshoff, M. Gonschior, High quality laser cutting of ceramics through adapted process techniques, Proc. SPIE 2062 (1993) 125–135.
- [4] B.S. Yilbas, R. Davies, Z. Yilbas, Study into the measurement and prediction of penetration time during the CO₂ laser cutting process, Proc. Inst. Mech. Eng. J. Eng. Manuf., B 204 (1990) 105–113.
- [5] K.M. Lam, Laser profiling-intricity factor, Beng. dissertation, Heriot-Watt University, Edinburgh, UK, 1992.
- [6] G.A. Thomson, The development of CO₂ laser cutting material evaluation procedure and the construction of a database to store this information, Mphil. thesis, Heriot-Watt University, Edinburgh, UK, 1993.
- [7] S.L. Chen, W.M. Steen, The theoretical investigation of gas assisted laser cutting, Proc. ICALEO '91 1722 (1992) 221–230.
- [8] H. Haferkamp, F.W. Bach, T. Vinke, H.-P. Wendroff, Laser beam cutting using water cooling, Schweiss. Schneid. 42 (12) (1990) 631–633.
- [9] G. Chryssolouris, J. Bredt, S. Kordas, E. Wilson, Theoretical aspects of a laser machine tool, Trans. ASME, J. Eng. Ind. 110 (1988) 65–70.
- [10] E.J. Barbero, G.H. Kaufmann, S.R. Idelsohn, Fracture analysis of a surface-coated ceramic by speckle photography and finite elements, Opt. Laser Technol. 22 (1990) 17–22.